Arabian Journal of Chemistry (2014) **xxx**, xxx–xxx

King Saud University

Arabian Journal of Chemistry

www.ksu.edu.sa
www.sciencedirect.com

ORIGINAL ARTICLE

Synthesis, spectral analysis and study of antimicrobial activity of 2,5-diformyl-1*H*-pyrrole bis(methan-1-yl-1-ylidene)dimalonohydrazone

Poonam Rawat, R.N. Singh *

Department of Chemistry, University of Lucknow, Lucknow 226007, U.P., India

Received 24 July 2014; accepted 29 October 2014

KEYWORDS

NMR spectroscopy;
IR spectroscopy;
DFT;
NBO

Abstract We have synthesized 2,5-diformyl-1*H*-pyrrole bis(methan-1-yl-1-ylidene)dimalonohydrazone (DPBMD) and characterized by elemental analysis, FT-IR, UV–Vis, Mass, ^{1}H and ^{13}C NMR spectroscopy. Theoretical calculations were performed by *ab initio* RHF and density functional theory (DFT)/B3LYP method, 6-31G(d,p) and 6-311++G(d,p) basis sets. The calculated scaled vibrational frequency values have been compared with experimental FT-IR spectrum. The calculated result shows excellent agreement between experimental and calculated frequencies at B3LYP method and 6-311++G(d,p) basis set. The thermodynamics properties, NBO, nonlinear optical properties and mulliken charges of DPBMD have also been analyzed. Involvement of nitrogen [N8/N18] and [N14/N24] lone pairs of electron with [π^*(C9–O10), π^*(C6–N7)/π^*(C16–N17), π^*(C19–O20)] and [(π^*(C12–O13)/π^*(C22–O23)] leads to an enormous stabilization of 84.6/84.6 and 64.1/64.1 kcal/mol of the molecule. A combined experimental and theoretical stretching wavenumber symmetric (3003, 3332 cm^{-1}) and asymmetric (3276, 3398 cm^{-1}) analysis confirms free NH_2 groups in DPBMD. The calculated first hyperpolarizability ($\beta_0 = 5.80 \times 10^{-30}$ esu) at B3LYP method and 6-311++G(d,p) basis sets indicates that DPBMD can be used as an attractive material for non-linear optical. The electronic descriptor analysis indicates that DPBMD is a good precursor for heterocyclic synthesis and as ligand for metal complex formation. The preliminary bioassay suggested that the DPBMD compound exhibits relatively good antibacterial and fungicidal activity against *Escherichia coli*, *Pseudomonas aeruginosa*, *Staphylococcus aureus*, *Streptococcus pyogenes*, *Candida albicans*, and *Aspergillus niger*.

* Corresponding author. Tel.: +91 9451203805.
E-mail address: rnsvk.chemistry@gmail.com (R.N. Singh).
Peer review under responsibility of King Saud University.

Production and hosting by Elsevier

1. Introduction

Pyrrole is the simplest example of azole heterocyclic compound that contains nitrogen as a one heteroatom. Pyrrole is unique among the five-membered mono heterocyclic aromatic

http://dx.doi.org/10.1016/j.arabjc.2014.10.050
1878-5352

Please cite this article in press as: Rawat, P., Singh, R.N. Synthesis, spectral analysis and study of antimicrobial activity of 2,5-diformyl-1*H*-pyrrole bis(methan-1-yl-1-ylidene)dimalonohydrazone. Arabian Journal of Chemistry (2014), http://dx.doi.org/10.1016/j.arabjc.2014.10.050

compounds having electron-releasing ability through resonance. The bis-hydrazones of dicarbonyl compounds are of interest primarily due to their high complexing ability (Balasubramanian et al., 2010; Leonid et al., 2009; Alamuoye and Nwabueze, 2014; John et al., 1967; Zoubi et al., 2012) as well as various biological activity (Alamuoye and Nwabueze, 2014; John et al., 1967) and material applications (Zoubi et al., 2012). Previously, a wide series of hydrazones of 2- and 4-formylpyrrole have been synthesized and studied (Alonso et al., 2002; Safoklov et al., 2002; Wardell et al., 2006), while the data on bis-hydrazones of 2,5-diformyl-1*H*-pyrrole are less (Bacchi et al., 1998; Popov et al., 2013).

It is well known that mono- and bishydrazones or dihydrazide–hydrazone find wide application in medicine as active physiological preparations. The Bishydrazones or dihydrazide–hydrazone are potential polyfunctional ligand or ditopic ligand and find wide application in coordination chemistry (Balasubramanian et al., 2010; Popov et al., 2009; Alamuoye and Nwabueze, 2014; John et al., 1967; Zoubi et al., 2012, Battaglia et al., 1990). The dihydrazide–hydrazones are capable of giving rise to monometallic (Adam, 2014), homobimetallic (Lal et al., 2010) and heterobimetallic (Lal et al., 2004) complexes.

Pyrrole dihydrazones and their metal complexes have attracted great attention and growing interest due to their interesting biological properties-antibacterial, antifungal and antitumor activities and material applications. These compounds have been found to have therapeutic activity for example in the treatment of tuberculosis and Fe overload disease (Alamuoye and Nwabueze, 2014; John et al., 1967; Zoubi et al., 2012). They are useful as fluorescent materials, pigments, and analytical reagents and polymer-coating. The presence of two coordinating unit in dihydrazide–hydrazones ligands may yield supramolecular architectures and better coordinative properties than those a sole coordinative unit (Adam, 2014; Lal et al., 2010, 2004). Among the research dealing with complexes of hydrazones, increasing attention has been devoted to metal complexes in view of chemical properties, biological significance, industrial importance, and structural variety of metal complexes. Since biocidal properties of metal complexes of dihydrazones are dependent on the organic group and the ligand attached to metal, an interesting development is introducing ligand which is bioactive.

However, less attention has been paid on study of acid dihydrazide of diformylpyrrole derivatives. There are possibility of formation of several products depending on ratio of reactants 2,5-diformyl-1*H*-pyrrole and acid dihydrazide as well as used solvents and reaction conditions. In view points of above literature survey, the objectives of the present investigation are synthesis, structural elucidation, spectral characterization, biological activity and other properties of 2,5-diformyl-1*H*-pyrrole bis(methan-1-yl-1-ylidene)dimalonohydrazone. This compound will provide opportunity for synthesis of new heterocyclic compounds and metal complexes that may have considerable pharmacological activities and material applications.

2. Experimental details

2.1. Physical measurement

All chemicals were used of analytical grade and procured from Sigma–Aldrich. TLC analysis was carried out using glass plates pre-coated with silica gel (Kieselgel 60 F256, 0.2 mm, Merck). The ^{1}H and ^{13}C NMR spectra of the studied compound were recorded in DMSO-d6 on Bruker DRX-300 spectrometer using TMS as an internal reference. The Mass spectrum (MS) of the studied compound was recorded on JEOL-Acc TDF JMS-T100LC, Accu TOF mass spectrometer. The FT-IR spectrum was recorded in KBr medium on a Bruker spectrometer. The UV–Visible absorption spectrum of the studied compound, (1×10^{-6} M in DMSO) was recorded on ELICO SL-164 spectrophotometer.

2.2. Preparation of malonodihydrazide (malonic acid hydrazide)

A solution of hydrazine hydrate (0.1562 g, 0.15 ml, 3.122 mmol) in 10 ml ethanol was added dropwise with stirring in solution of diethyl malonate (0.500 g, 0.47 ml, 3.122 mmol) in 10 ml ethanol. Reaction mixture was refluxed for overnight. After refluxing, white precipitate was obtained. The precipitate was filtered off, washed with methanol and dried in air. Color: white; Yield: 0.2922 g, 70.85%; m.p.: 147 °C.

2.3. Synthesis of 2,5-diformyl-1H-pyrrole bis(methan-1-yl-1-ylidene)dimalonohydrazone (5 = DPBMD)

2,5 Diformyl-1*H*-pyrrole was prepared by the literature procedure (Knizhnikova et al., 2007). The reaction mixture of 2,5 diformyl-1*H*-pyrrole (0.150 g, 1.219 mmol) and malonic acid dihydrazide (0.322 g, 2.438 mmol) in ratio 1:2 in Water/Ethanol (5:0.5) solution was refluxed for 10 min giving light yellow color to the reaction solution and completion of reaction was analyzed using thin layer chromatography (TLC). TLC analysis was carried out using glass plates pre-coated with silica gel (Kieselgel 60 F256, 0.2 mm, Merck). The product was separated by column chromatography on silica using hexane and ethylacetate as eluent. Thus pure light yellow color product was obtained along with other side products. Color: Light yellow, Yield: 50%. Elemental analysis for $C_{12}H_{17}N_9O_4$: calcd C 41.02, H 4.88, N 35.88; obs. C 41.00, H 4.90, N 35.80. ^{1}H NMR (300 MHz, DMSO-d_6): δ 11.623 (s, 1H, pyrrolic NH), 12.223 (s, 2H, hydrazine–NH), 8.884 (s, 2H, azomethine ─CH═N─), 4.229 (s, 4H, CH_2), 6.346–6.363 (d, 2H, pyrrolic ring CH), 5.849 (s, 4H, NH_2). The MS for $C_{12}H_{17}N_9O_4$: calcd 351.32 amu, found m/z 352.26 [$M+H^+$].

2.4. Synthesis of macrocyclic bis-hydrazone of pyrrole (6)

The reaction mixture of 2,5 diformyl-1*H*-pyrrole (0.150 g, 1.219 mmol) and malonic acid dihydrazide (0.161 g, 1.219 mmol) in ratio 1:1 was taken in methanol with small amount of conc. HCl. The reaction was refluxed for 10 h, turmeric yellow color precipitate was obtained. Color: Turmeric yellow, Yield: 65%. Solubility: Poor solubility in organic solvents. Elemental analysis, ^{1}H NMR and Mass spectra of the formed macrocyclic bis-hydrazone (6) are reported as: Elemental analysis for $C_{18}H_{18}N_{10}O_4$ calcd C 49.31, H 4.14, N 31.95; obs. C 49.00, H 4.71, N 31.87. ^{1}H NMR (300 MHz, DMSO-d_6): δ 11.806 (s, 2H, pyrrolic NH), 11.106 (s, 4H, hydrazone–NH), 8.787 (s, 4H, azomethine CH═N─), 4.538 (s, 4H, CH_2), 6.830–6.840 (d, 4H, pyrrolic ring CH), NH_2 singlet peak observed. The MS for $C_{18}H_{18}N_{10}O_4$ calcd 438.15 amu, found m/z 439.25 [$M+H^+$].

Please cite this article in press as: Rawat, P., Singh, R.N. Synthesis, spectral analysis and study of antimicrobial activity of 2,5-diformyl-1*H*-pyrrole bis(methan-1-yl-1-ylidene)dimalonohydrazone. Arabian Journal of Chemistry (2014), http://dx.doi.org/10.1016/j.arabjc.2014.10.050

2.5. Computational details

Gaussian 09 program package (Frisch et al., 2010) is used to predict the molecular structure and spectroscopic analysis of the compound using HF and B3LYP method at 6-31G(d,p) and 6-311++G(d,p) basis set. Potential energy curves for DPBMD were obtained by calculating the variation of total energy versus the following dihedral angles (C3C2C6N7/C4C5C16N17), (C9C11C12N14/C19C21C22N24) and (C6N7N8C9/C16N17N18C19). For this purpose the calculations were performed with DFT by using B3LYP functional and 6-311++G(d,p) basis set. The dihedral angles were varied from 0° to 360° with an interval of 10°. Harmonic vibrational wavenumbers have been calculated using analytic second derivatives to confirm the convergence to minima on the potential energy surface and to evaluate the zero-point vibrational energy. Normal coordinate analysis on DPBMD has been performed to obtain full description of the molecular motion pertaining to the normal modes. The ^{1}H and ^{13}C nuclear magnetic resonance (NMR) chemical shifts calculations have been performed using gauge-invariant atomic orbital (GIAO) method (Ditchfield, 1972; Wolinski et al., 1990) at HF and B3LYP level with 6-31G(d,p) and 6-311++G(d,p) basis set. The ^{1}H isotropic chemical shifts were referenced to the corresponding values for TMS, which was calculated at the same level of theory. Chemical shift of any 'x' proton (δ_X) is equal to the difference between isotropic magnetic shielding (IMS) of TMS and proton (x). It is defined by the equation: $\delta_X = IMS_{TMS} - IMS_X$. The effect of solvent on the theoretical NMR parameters was evaluated using the integral equation formalism polarizable continuum model (IEFPCM) model (Tomasi et al., 2005). The electronic properties; HOMO–LUMO energies, absorption wavelengths and oscillator strengths are calculated using HF and B3LYP method of the time-dependent DFT (TD-DFT) (Wang, Yi-Gui, 2009), basing on the optimized structure in gas phase

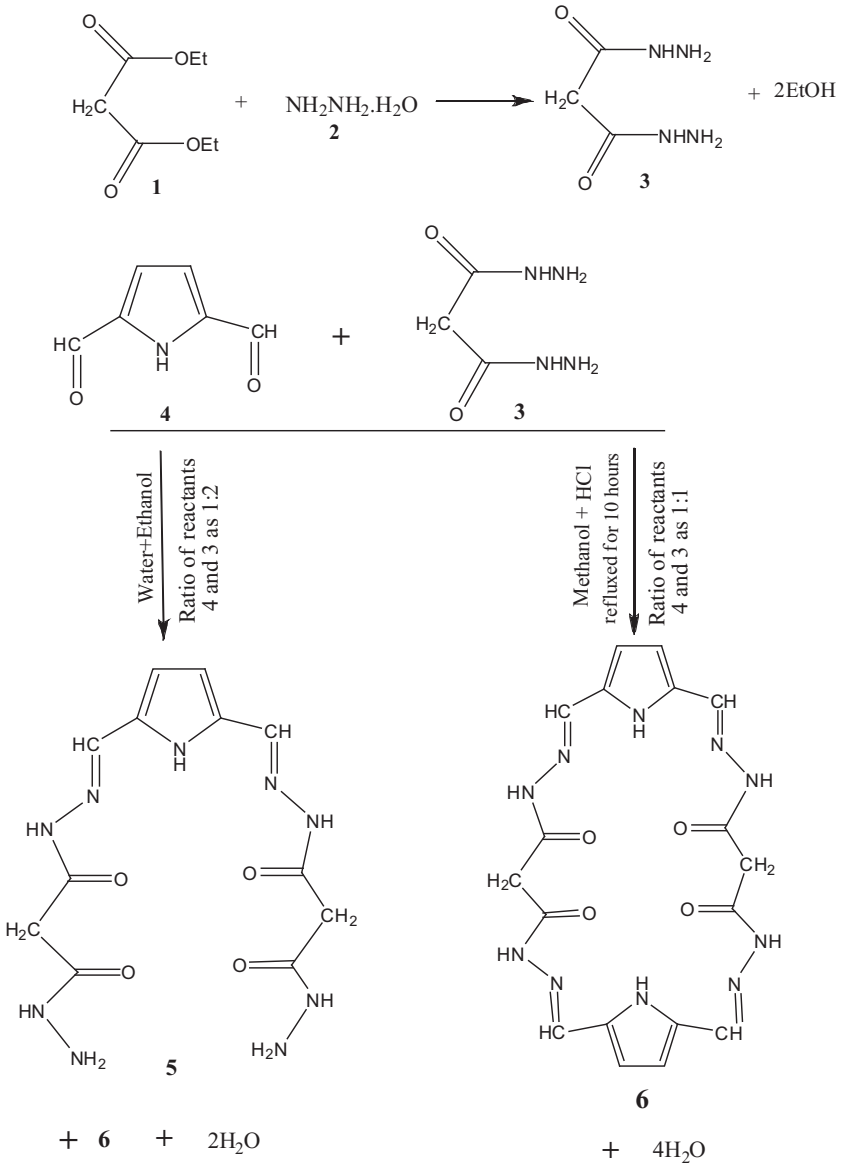

Scheme 1 The route for the formation of (**5** = DPBMD) and **6**.

and solvent phase (Dimethyl sulfoxide (DMSO)) using IEFPCM model (Tomasi et al., 2005). DMSO with relative permittivity (ε) 46.7 was used as solvents in both calculations of NMR and TDDFT. Natural bond orbital (NBO) analysis is performed to gain a better understanding of the charge distribution within molecule (Weinhold and Landis, 2005). Potential energy distribution along internal coordinates is calculated by Gar2ped software (Martin et al., 1995). Topological parameters are calculated using software AIMALL (Version 10.05.04) (Bader et al., 2000). The optimized geometries of the molecule are visualized using Gauss–View software (Gauss-View, 2003). To reveal chemical reactivity of the molecule, the molecular electrostatic potential surface (MEP), for the 0.002 a.u. isosurfaces of electron density, is plotted over the optimized geometry of conformer I of studied molecule. The total static dipole moment (μ_0), the mean polarizability ($|\alpha_0|$), the anisotropy of the polarizability ($\Delta\alpha$) and the total static first hyperpolarizability (β_0) using x, y, z components are defined as using Eqs. (1)–(4) (Jug et al., 2003) and presented as:

$$\mu = (\mu_x^2 + \mu_y^2 + \mu_z^2)^{1/2} \quad (1)$$

$$|a_0| = 1/3(a_{xx} + a_{yy} + a_{zz}) \quad (2)$$

$$\Delta a = 2^{-1/2}[(a_{xx} - a_{yy})^2 + (a_{yy} - a_{zz})^2 + (a_{zz} - a_{xx})^2]^{1/2} \quad (3)$$

$$\beta_0 = (\beta_x^2 + \beta_y^2 + \beta_z^2)^{1/2} \quad (4)$$

where, $\beta_x = \beta_{xxx} + \beta_{xyy} + \beta_{xzz}; \beta_y = \beta_{yyy} + \beta_{xxy} + \beta_{yzz}; \beta_z = \beta_{zzz} + \beta_{xxz} + \beta_{yyz}$.

2.6. Antimicrobial activity

The compound (DPBMD), reactant: 2,5-diformyl-1*H*-pyrrole and malonic acid dihydrazide were dissolved in DMSO. Proper drug controls were used. All compound and reactants were taken at concentration of 100 and 200 μg/ml for testing antibacterial activity and antifungal activity. The compound diffused into the medium produced a concentration gradient. After the incubation period, the zones of inhibition were measured in mm. The tabulated results represent the actual readings control. The compound was tested against *Escherichia coli*, *Pseudomonas aeruginosa (gram negative bacteria)*, *Staphylococcus aureus*, *Streptococcus pyogenes (gram positive bacteria)*, *Candida albicans* and *Aspergillus niger (fungi)*. The plates were placed in an incubator at 37 °C within 30 min of preparation for bacteria and 22 °C for fungal. After 48 h incubation for bacteria and 7-days for fungal, the diameter of zone (including the diameter disk) was measured and recorded in mm. The measurements were taken with a ruler, from the bottom of the plate, without opening the lid.

3. Results and discussion

3.1. Synthesis

There are possibility of formation of products such as 2,5-diformyl-1*H*-pyrrole bis(methan-1-yl-1-ylidene)dimalonohydrazone (DPBMD), macrocycle and polymeric products, depending on ratio of reactants 2,5-diformyl-1*H*-pyrrole (4) and malonic acid dihydrazide (3) as well as used solvents and reaction conditions. The general route for synthesis of

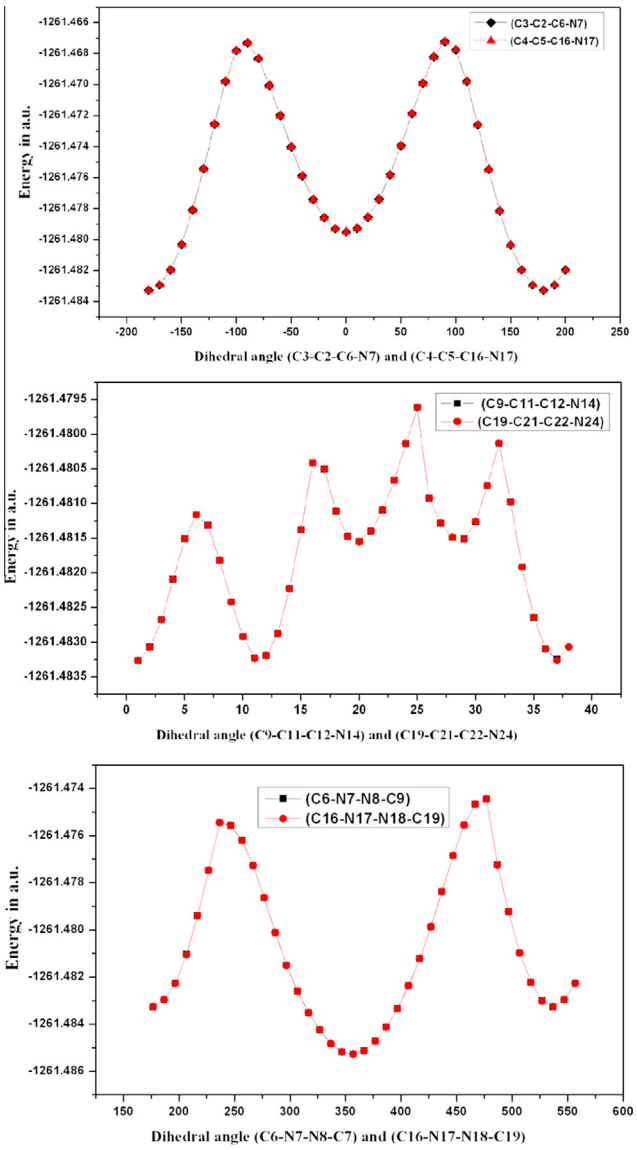

Figure 1 Potential surface scan curve for DPBMD.

DPBMD (5) and (6) are shown in Scheme 1. When 2,5-diformyl-1*H*-pyrrole react with malonic acid dihydrazide in a stoichiometric ratio of 1:2, compound 2,5-diformyl-1*H*-pyrrole bis(methan-1-yl-1-ylidene)dimalonohydrazone (5 = DPBMD), is formed as major product along with (6) as minor. If 2,5-diformyl-1*H*-pyrrole was reacted with malonic acid dihydrazide in stoichiometric ratio of 1:1, a macrocyclic dipyrrolic dimalonohydrozone compound or macrocyclic bis-hydrazone (6) was obtained. The macrocyclic bis-hydrazone (6) has poor solubility in most of the organic solvents. Therefore, the spectral analysis, biological activity and all quantum chemical calculations have been performed on DPBMD compound.

3.2. Molecular geometry, conformational study, theoretical considerations on reaction thermodynamics and topological parameters at bond critical points (BCP) of DPBMD

After the establishment of the structure of the molecule with the help of ^{1}H, ^{13}C NMR and Mass spectrometry, optimization and

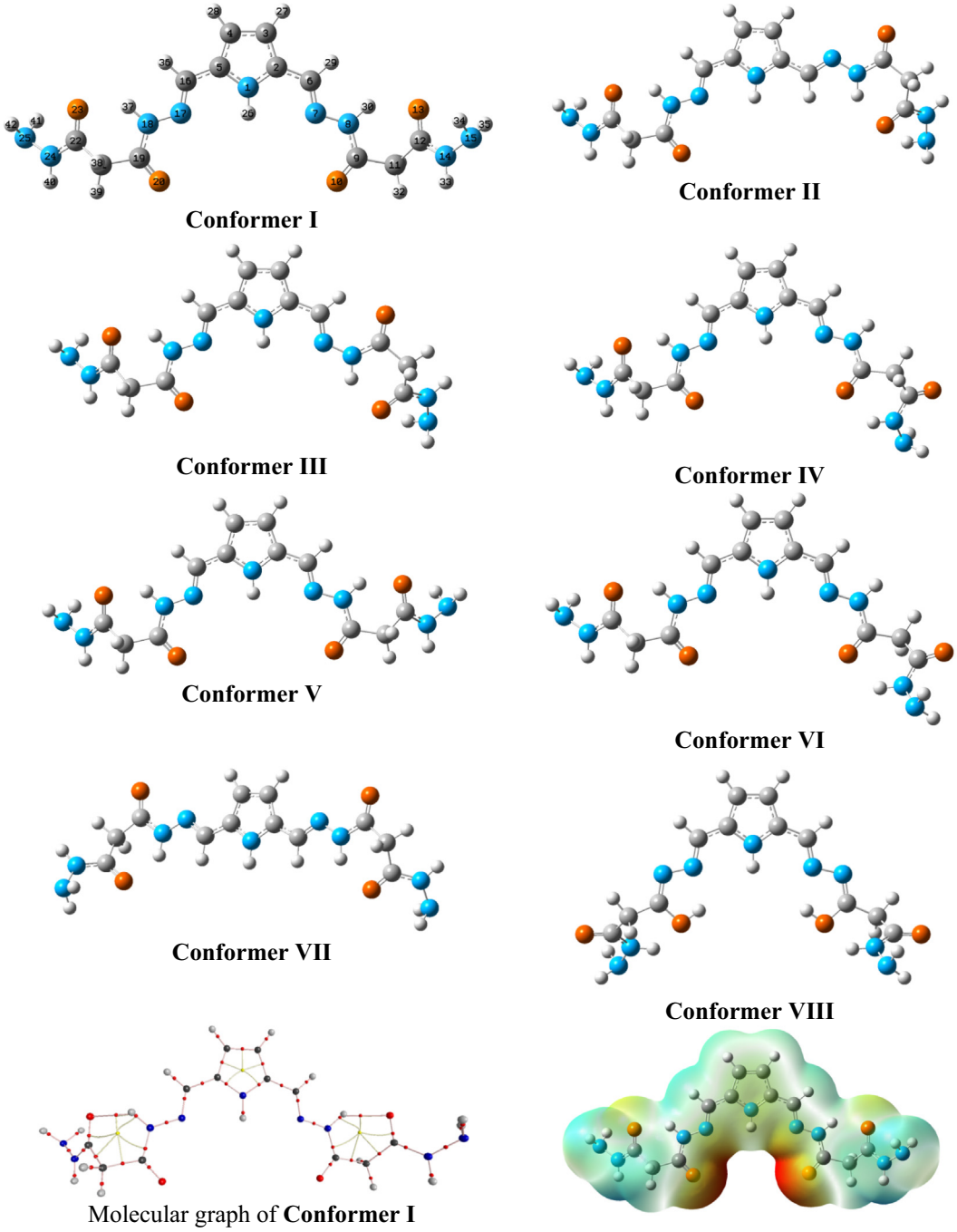

Figure 2 Optimized geometries of the conformers, molecular graph for conformer I of DPBMD and electrostatic potential surface map of Conformer I for DPBMD.

conformational studies have been conducted without imposing any symmetry constrains on the molecule DPBMD. The molecular geometry and conformational analysis plays a very important role in determining the structure–properties relationship. The potential energy surface (PES) is a central concept in computational chemistry. A PES is the relationship – mathematical or graphical – between the energy of a molecule (or a collection of molecules) and its geometry (Bruni et al., 2012). The PES curve for DPBMD has been shown in Fig. 1. Six separate potential energy surface scan have been done: (i) by rotating around dihedral angles (C3C2C6N7), (ii) (C4C5C16N17), (iii) (C9C11C12N14), (iv) (C19C21C22N24), (v) (C6N7N8C9), (vi) (C16N17N18C19). The same conformers have been obtained around the dihedral angles (C3C2C6N7) and (C4C5C16N17), (C9C11C12N14) and (C19C21C22N24), (C6N7N8C9) and (C16N17N18C19) which have been clearly seen from Fig. 1.

After the rotation of different groups, the minimum energy conformer I is obtained on potential energy surface curve. All calculations have been performed on lower energy conformer I

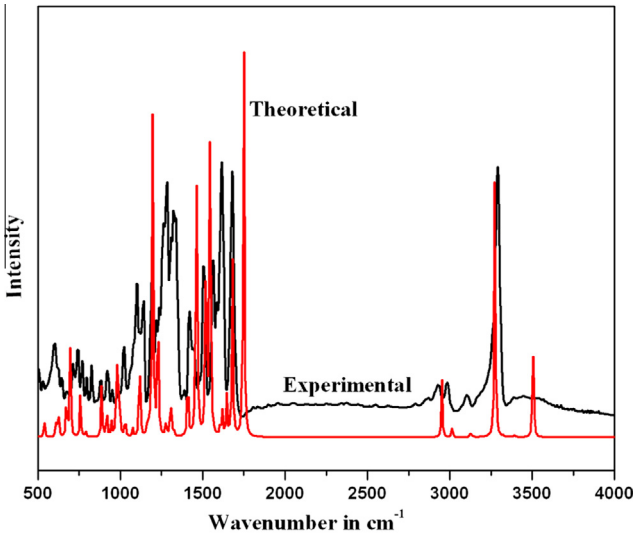

Figure 3 Comparison between experimental and theoretical FT-IR spectrum of Conformer I for DPBMD.

of DPBMD. The geometry of conformer I has been further optimized on HF/B3LYP/6-31G(d,p), B3LYP/6-31G(d,p) and B3LYP/6-311++G(d,p) level. The obtained conformers are shown in Fig. 2. The hydrazone molecule (conformer I) exists as the keto-amine tautomer with the configuration *E* across the azomethine bond. As for conformer I, the enol-imine tautomeric form is energetically more favorable. The difference between the energy of conformer I and VIII is equal to 20.81 kcal/mol, with preferred enol-imine form (conformer I). The keto-amine tautomer of conformer I acting as a ligand can coordinate in the multidentate mode during metal complex formation. The conformer I exist in *E* form and more stable than *Z* (conformer III). The conformer I is 7.977 kcal/mol more stable than conformer III. In conformer I two malonylhydrazide units are in *E*-configuration having lower energy conformer and also well reported in the crystal structure of dihydrazones derivatives (Eshkourfu et al., 2011; Sedaghat and Monajjemzadeh, 2011). The *E*-configuration about the Schiff base C6═N7 and C16═N17 bond. The symmetry in the N1─C5 and N1─C2 bond lengths is explained due to the delocalization of electron and presence of the two similar malonylhydrazide groups at C2 and C5 carbon atom of pyrrole ring. The energy difference between conformer (I and II), (I and IV), (I and V), (I and VI), (I and VII) have been found to be 11.597, 10.311, 9.2582, 10.333, 16.496 kcal/mol, respectively. The electron delocalization is extended on both the side of pyrrole ring toward carbonyl group. The optimized bond lengths, and bond angles calculated by using *ab initio* HF and DFT(B3LYP) methods with 6-31G(d,p)/6-311++G(d,p) basis set of DPBMD are shown in Supplementary Tables S1, S2 and S3. The Molecular structure of conformer I possesses C_1 point group symmetry. The optimized structural parameters (bond lengths, bond angles and dihedral angles) of lower energy conformation are comparable with experimentally obtained single crystal X-ray diffraction data (Popov et al., 2013). It has been seen that the DFT method give comparable geometries with experimental geometry, which differ from each other by not more than 0.037 Å in bond length and 2.2° in bond angles. The optimized geometries of conformer I of DPBMD calculated at HF and B3LYP method were compared by superimposing them using a least squares algorithm that minimizes the distances of the corresponding non-hydrogen atoms shown in Supplementary Fig. S1. The calculated bond lengths of DPBMD by HF method are shorter than DFT/B3LYP method and are comparable with experimental value in case of covalent bonds. The theory of AIM efficiently describes H-bonding, gives opportunity about an electron density region of a system and governs properties at BCP. Molecular graph of DPBMD using AIM program at B3LYP/6-31G(d,p) level is shown in Fig. 1. There are two intramolecular interactions in DPBMD.

3.3. Spectroscopic analysis

3.3.1. Vibrational analysis

A simulated IR spectrum of conformer I for DPBMD is shown in Fig. 3. The calculated vibrational wavenumbers are higher than their experimental values for the majority of the normal modes. The detailed vibrational assignment of the experimental wavenumbers is based on normal mode analyses and a comparison with theoretically scaled wavenumbers. The observed and scaled theoretical frequencies and modes of description calculated at B3LYP method and 6-311++G(d,p) basis set are listed in Table 1. The calculated wavenumbers at HF and, B3LYP method and 6-31G(d,p) basis set are shown in Supplementary Table S4. The calculated wavenumbers at HF/6-31G(d,p), B3LYP/6-31G(d,p) and B3LYP/6-311++G(d,p) level are scaled down using single scaling factor 0.9135, 0.9608, 0.970, respectively, to discard the anharmonicity present in real system (Ramalingam et al., 2010). In the experimental FT-IR spectrum of DPBMD, the N–H stretches of pyrrole (ν_{N-H}) are observed at 3289 cm^{-1}, whereas it is calculated as 3511, 3502, 3473 cm^{-1} at HF/6-31G(d,p), B3LYP/6-31G(d,p), B3LYP/6-311++G(d,p) level, respectively. According to Internal coordinate system recommended by Pulay et al. (1979), imino group (X–NH–Y) associate with four types of vibrational frequencies. In literature it is well reported that the NH stretching vibrations give rise to a strong band in the region 3390 ± 60 cm^{-1} (Silverstein and Webster, 1963). The calculated N–H stretches of NH_2-N**H**CH_2CON**H**– part of conformer I for DPBMD at 3540, 3374, 3374 cm^{-1} (HF/6-31G(d,p)), 3507, 3274, 3274 cm^{-1} (B3LYP/6-31G(d,p)), 3489, 3273, 3272 cm^{-1} (B3LYP/6-311++G(d,p)), correspond to the observe N–H stretch at 3318 and 3000 cm^{-1} in the experimental spectrum. The calculated scissoring mode of N–H amide part at 1672 (HF) 1646 (B3LYP/6-31G(d,p)) 1635 cm^{-1} (B3LYP/6-311++G(d,p)), matches well with the observed wavenumber at 1597 cm^{-1}. The rocking mode of N–H amide part calculated at 1286 (HF) 1303 (B3LYP/6-31G(d,p)) 1293 cm^{-1} (B3LYP/6-311++G(d,p). The wagging mode calculated at 980 (HF) 978 (B3LYP/6-31G(d,p)) 968 cm^{-1} (B3LYP/6-311++G(d,p) matches well with the observed wavenumber at 951 cm^{-1}. In the theoretical IR spectrum, the NH_2 asymmetric and symmetric stretching vibrations are assigned at 3453 (HF), 3393 (B3LYP/6-31G(d,p)), 3398 (B3LYP/6-311++G(d,p), 3405 (HF), 3324 (B3LYP/6-31G(d,p)), 3332 (B3LYP/6-311++G(d,p) cm^{-1}, respectively, with very low intensity. The weak band of NH_2 scissoring is assigned at 1504, 1472, 1452 cm^{-1} at HF/6-31G(d,p), B3LYP/6-31G(d,p), B3LYP/6-

Please cite this article in press as: Rawat, P., Singh, R.N. Synthesis, spectral analysis and study of antimicrobial activity of 2,5-diformyl-1*H*-pyrrole bis(methan-1-yl-1-ylidene)dimalonohydrazone. Arabian Journal of Chemistry (2014), http://dx.doi.org/10.1016/j.arabjc.2014.10.050

Table 1 Theoretical (selected) and experimental vibrational wavenumbers of Conformer I for DPBMD and their assignments at B3LYP/6-311 + + G(g,p) level: Wavenumbers ($\bar{V}$/cm).

Mode No.	Theoretical $\bar{V}$	Exp	Assignment (PED) ⩾ 5%
120	3489	3481	ν(N14H33)(91) + ν(N24H40)(8)
119	3489	3318	ν(N24H40)(92) − νas(N14H33)(8)
118	3473	3289	ν(N1H26)(99)
117	3398	3276	νas(N25H42)(51) − νas(N25H41)(49)
116	3398	3108	ν(N15H35)(51) − ν(N15H34)(49)
115	3332	3003	ν(N25H41)(51) + ν(N25H42)(49)
114	3332		ν(N15H34)(51) + ν(N15H35)(49)
113	3273		ν(N8H30)(56) + νas(N18H37)(43)
112	3272	3000	ν(N18H37)(56) − ν(N8H30)(43)
111	3115	2939	νPy(C3H27)(49) + νPy(C4H28)(49)
110	3101		νPy(C4H28)(50) − νasPy(C3H27)(50)
109	2993	2990	ν(CH2)(78) + ν(CH2)
108	2993		ν(CH2)(78) − νas(CH2)(40)
107	2931		ν(C6H29)(50) + ν(C16H36)(49)
106	2931		ν(C16H36)(50) − νas(C6H29)(49)
105	2921		ν(CH2)(86) + ν(CH2)(11)
104	2921		ν(CH2)(86) + ν(CH2)(11)
103	1705	1679	ν(C═O)(38) + ν(C═O)(38)
102	1696		ν(C═O)(38) − νas(C═O)(38)
101	1646		ν(C═O)(48) + ν(C═O)(25) − νas(C12N14)(5)
100	1646	1618	ν(C═O)(48) − νas(C═O)(25) − νas(C38N24)(5)
99	1635	1597	δsc(N14H33)(46) − δsc(N24H40)(26) + ρ(N14H33)(19)
98	1635		δsc(N24H40)(61) + δsc(N14H33)(21) + ρ(N14H33)(9)
97	1599	1586	ν(C16═N17)(27) − νas(C6═N7)(27) − νas(C5C16)(8) + ν(C2C6)(8) − ρ(C16═N17)(6) + ρ(C6═N7)(6)
96	1587	1563	ν(C6═N7)(31) + ν(C16═N17)(31) − ρ(C16═N17)(7) − ρ(C16═N17)(7) − νas(C2C6)(6) − νas(C6═N7)(6)
95	1535		δsc(N7N8)(10) + ν(PyC4C5)(9) − νas (PyCC)(9) + δs(C19N18)(9) − νas(C16═N17)(8) + ν(C6═N7)(8) − δas(PyCH)(5) + ρ(C19N18)(5)
94	1534		δsc(N7N8)(20) − δas(C19N18)(20) − ρ(C19N18) (8) + ρ(N7N8)(7) + ν(N8C9)(6) + ν(N18C19)(6)
93	1509	1506	δs(C19N18)(18) + δsc(N7N8)(16) + ρ(N7N8)(7) δ(PyCH)(6) + ρ(C19N18)(6) + ν(N8C9)(5) − νas(N18C19)(5) − ν(PyC4C5)(5)
92	1458	1440	δ(Pyring)(10) − νas(C6═N7)(10) − νas(C2C6)(10) − νas(PyC3C2) (8) + (PyC4C5)(8)
91	1452		ρ(NH2)(23) − δsc(NH2)(21) − νas(C22N24)(13) + ν(C12N14)(12) − ρ(NH2)(9)
90	1451	1451	ρ(NH2)(21) + δsc(NH2)(17) + ν(C12N14)(11) + ν(C38N24)(11) + ρ(NH2)(8)
89	1400		δsc(CH2)(21) − δsc(CH2)(20) − νas(PyNC)(12) + ν(PyNC)(12) + δas(PyCH)(6) + ν(PyCC)(5)
88	1400	1420	δsc(CH2)(43) + δsc(CH2)(42)
87	1390		δsc(CH2)(21) − δsc(CH2)(19) − νas(PyNC)(13) + ν(PyNC)(13) − δas(PyCH)(6) ν(PyCC)(5)
86	1389	1339	ν(PyCC)(15) + ν(PyC4C5)(15) − νas(PyNC)(14) − νas(PyNC)(14) − ρ(N7N8)(6) − ρ(C16═N17)(6)
85	1318	1323	ρ(C16═N17)(27) − ρ(N7N8)(27) + ν(C16═N17)(5) − νas(C6═N7)(5)
84	1305	1306	ν(PyCC)(38) − δas(PyCH)(7) + δ(PyCH)(7) − νas(PyCC)(6) − νas(PyC4C5)(6) + ν(PyNC)(5) + ν(PyNC)(5)
83	1302		ρ(CH2)(14) + ω(CH2)(12) − δsc(NH2)(10) − ρ(NH2)(8) − ν(C21C22)(7) − νas(C11C12)(6)
82	1302	1301	ω(CH2)(14) − ρ(CH2)(12) − ρ(NH2)(9) + δsc(N24H40)(9) − νas(C11C12)(7) ν(C21C22)(6)
81	1293	1283	ρ(NH2)(83) + ρ(N14H33)(8)
80	1293		ρ(N14H33)(62) + δsc(N14H33)(17) − ρ(NH2)(10) + ω(N14H33)(5)
79	1268	1262	ρ(N7N8)(28) + ρ(C16═N17)(28) + ν(PyC4C5)(13) + ν(PyC4C5)(6) + ν(PyC2C3)(6)
78	1226		ρ(CH2)(22) + ω(CH2)(21) + ν(N24N25)(8) + δsc(NH2)(6) − νas(C38N24)(5) − νas(C12N14)(5)
77	1226	1216	ω(CH2)(22) − ρ(CH2)(21) + ν(N14N15)(9) − νas(N24N25)(8) − δsc(N24H40)(5) − νas(C12N14)(5) + ν(C38N24)(5)
76	1221	1192	δ(PyCH)(43) − δas(PyCH)(12) − δas(PyCH)(12)
75	1188		ν(N18C19)(15) + ν(N8C9)(15) − νas(C19C21)(9) − νas(C9C11)(9) − δsc(N7N8)(5)

(*continued on next page*)

Please cite this article in press as: Rawat, P., Singh, R.N. Synthesis, spectral analysis and study of antimicrobial activity of 2,5-diformyl-1*H*-pyrrole bis(methan-1-yl-1-ylidene)dimalonohydrazone. Arabian Journal of Chemistry (2014), http://dx.doi.org/10.1016/j.arabjc.2014.10.050

Table 1 (*continued*)

Mode No.	Theoretical $\bar{V}$	Exp	Assignment (PED) ⩾ 5%
74	1185		ν(N8C9)(15) − vas(N18C19)(15) − vas(C9C11)(8) + ν(C19C21)(8) − δsc(N7N8)(5)
73	1166		δ(PyCH)(13) + δ(PyCH)(13) + ν(C2C6)(11) − vas(C5C16)(11) − ρ(N7N8)(8) + ρ(C16═N17)(8) + δ(PyCH)(6)
72	1155	1142	70(20) 93(19) − vas(N24N25)(9) − vas(N14N15)(9) ρ(CH2)(6) + ω(N14H33)(6) + ω(CH2)(6) − ω(NH2)(5)
71	1152		70(15) − 93(15) + ν(N14N15)(9) − vas(N24N25)(9) + ω(N14H33)(6) + ρ(CH2)(5) − ω(CH2)(5) − ω(NH2)(5)
70	1102	1101	ν(N17N18)(20) + ν(N7N8)(19) − t(CH2)(6) − t(CH2)(6) − vas(C38N24)(5) − vas(C12N14)(5)
69	1096	1075	ν(N7N8)(17) − vas(N17N18)(17) + t(CH2)(7) − t(CH2)(7) − vas(C12N14)(5)
68	1060		ν(N17N18)(13) + ν(N7N8)(12) + t(CH2)(12) + t(CH2)(10) ν(C22N24)(5) + ν(C12N14)(5)
67	1060		ν(N7N8)(15) − vas(N17N18)(14) + t(CH2)(10) − t(CH2)(9) + ν(C12N14)(5) − vas(C22N24)(5)
66	1018	1022	δ(PyCH)(32) − δas(PyCH)(32) + ν(PyCC)(25)
65	993		δ(Pyring)(24) − vas(PyNC)(8) − vas(PyNC)(8) − vas(PyCC)(6)
64	986		ν(PyNC)(16) − vas(PyNC)(16) − δas(PyCH)(12) − δas(Pyring)(6)
63	968		ν(C21C22)(12) + ν(C11C12)(12) + ω(NH2)(11) + ω(N14H33)(11) − vas(N24N25)(10) − vas(N14N15)(9)
62	968	951	ν(C11C12)(13) − vas(C21C22)(12) + ω(N14H33)(11) − ω(NH2)(10) − vas(N14N15)(10) + ν(N24N25)(9)
61	943		δ(Pyring)(13) + ν(C19C21)(11) + ν(C9C11)(11) + ρ(C═O)(6) + ρ(C═O)(5)
60	942		ν(C9C11)(12) − vas(C19C21)(11) + δ(Pyring)(10)ρ(C═O)(7)
59	917	921	ω(CH2)(25) + ρ(CH2)(19) + ω(NH2)(5) + ω(N14H33)(5)
58	917	910	ω(CH2)(23) − ρ(CH2)(20) + ω(N14H33)(5) + ω(NH2)(5)
57	910	906	δoop(C16N17)(47) − δoop(C6N7)(47)
56	908	882	ω(C6N7)(45) + ω(C16N17)(45)
55	872		ω(N14H33)(19) − vas(N14N15)(14) + ω(NH2)(13) − vas(N24N25)(10)
54	872		ω(NH2)(20) − vas(N24N25)(14) + ω(N14H33)(13) + ν(N14N15)(10) − ω(CH2)(5)
53	827	826	δ(O23C22N24)(40) − ω(C3C4C2H27)(40) + τ(Pyring)(15)
52	792	796	δ(Pyring)(33) − δas(C6N7)(7) + δ(C5C16N17)(7)
51	776		t(CH2)(20) − ω(C═O)(8) − ω(C═O)(8) δs(C═O)(6) + δ(O23C24C22)(6) + ρ(C═O)(5)
50	765	769	δ(Pyring)(17) + δ(CH2)(9) − δas(CH2)(8) + ω(C═O)(7) − ω(C═O)(7)
49	751		ω(C3C4C2H27)(37) + δ(O23C22N24)(37) + τ(Pyring)(10) − ω(Pyring)(9)
48	726	713	δ(Pyring)(22) − δas(C6N7)(7) − δas(C5C16N17)(7) + δ(C6N7N8)(6) + δ(C16N17N18)(6) + ν(PyNC)(6) + ν(PyNC)(6)
47	685	674	ω(C19N17N18H37)(32)H30N8)(30) + ω(C═O)(5)–ω(C═O)(5) + ω(C9N7 H30N8)(30) + ω(C═O)(5) − ω(C═O)(5)
46	683		ω(C9N7H30N8)(31) − ω(C19N17N18H37)(29) − ω(C═O)(6) − ω(C═O)(5)
45	668		τ(Pyring)(56) + ω(C6N1C2C3)(16) + ω(C16C4N1C5)(16)
44	666		ω(C9N7H30N8)(10) + ω(C19N17N18H37)(10) − ρ(C═O)(9) − vas(C19C21)(6) + ν(C9C11)(6) − δas(O23C24C22)(5) + δs(C═O)(5) − δas(O20C19C21)(5)
43	666		ρ(C═O)(10) − ω(C9N7H30N8)(9) + ω(C19N17N18H37)(9) − vas(C9C11)(6) − vas(C19C21)(6) − δas(O20C19C21)(6) − δas(O23C24C22)(6) + ρ(C═O)(6)
42	634		τ(Pyring)(59) − ω(C6N1C2C3)(14) + ω(C16C4N1C5)(14)
41	622		ω(C═O)(18) − ω(C═O)(17) + ω(C21C19O20N18)(12) ω(C19N17N18H37)(11) − ω(C9N7H30N8)(10)
40	621		ω(C═O)(17) + ω(C═O)(16) − ω(C11C9O10N8)(12) ω(C21C19O20N18)(11) + ω(C9N7H30N8)(1) − ω(C19N17N18H37)(10)
39	606	600	ω(Pyring)(60) + τ(Pyring)(21)
38	542		ω(C21C19O20N18)(14) + ω(C11C9O10N8)(14) − ω(C19N17N18H37)(9) − ω(C9N7H30N8)(9)110(7) + ω(CH2)(7) − ρ(CH2)(6)
37	537	531	ω(C11C9O10N8)(15) − ω(C21C19O20N18)(14) − ω(C9N7H30N8)(10) ω(C19N17N18H37)(9)110(8) − ω(CH2)(7) − ρ(CH2)(6)
36	488	490	δ(C16C5)(10) + δ(C6C2)(10) + ρ(C═O)(7) + δ(O20C19C21)(6)
35	464		δ(C22N25H40C24)(11) − ω(O13N14N15C22)(11) − δas(O20C19C21)(8) − δas(Pyring)(6) − δas(C6N7)(6)
34	453		δ(C22N25H40C24)(30) + ω(O13N14N15C22)(28) − ω(C═O)(12) ω(C═O)(12)
33	441		ω(O13N14N15C22)(27) − δas(C22N25H40C24)(25) + ω(C═O)(11) ω(C═O)(10)
32	420		δ(C6N7N8)(14) + δ(C16N17N18)(14) − δas(O20C19C21)(8)

Proposed assignment and potential energy distribution (PED) for vibrational modes: Types of vibrations: ν-stretching, δsc-scissoring, ρ-rocking, ω-wagging, δ-deformation, δs-symmetric deformation, δas-asymmetric deformation, δip-in-plane deformation, δoop-out-of-plane deformation, τ-torsion, Pyring-pyrrole ring.

Please cite this article in press as: Rawat, P., Singh, R.N. Synthesis, spectral analysis and study of antimicrobial activity of 2,5-diformyl-1*H*-pyrrole bis(methan-1-yl-1-ylidene)dimalonohydrazone. Arabian Journal of Chemistry (2014), http://dx.doi.org/10.1016/j.arabjc.2014.10.050

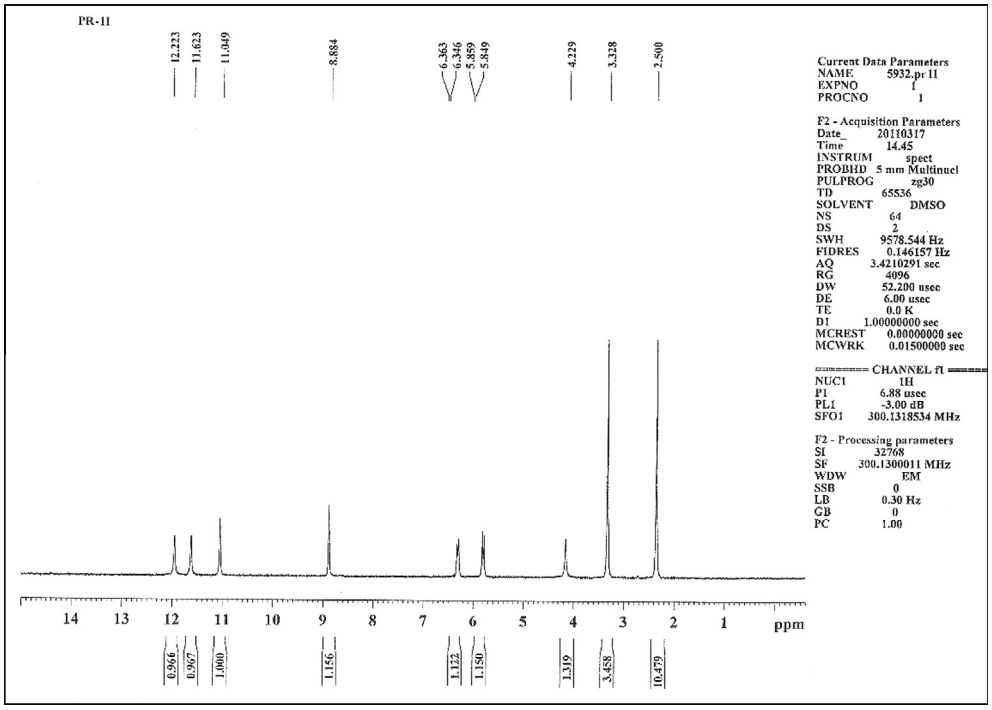

Figure 4 Experimental ^{1}H NMR spectrum of DPBMD.

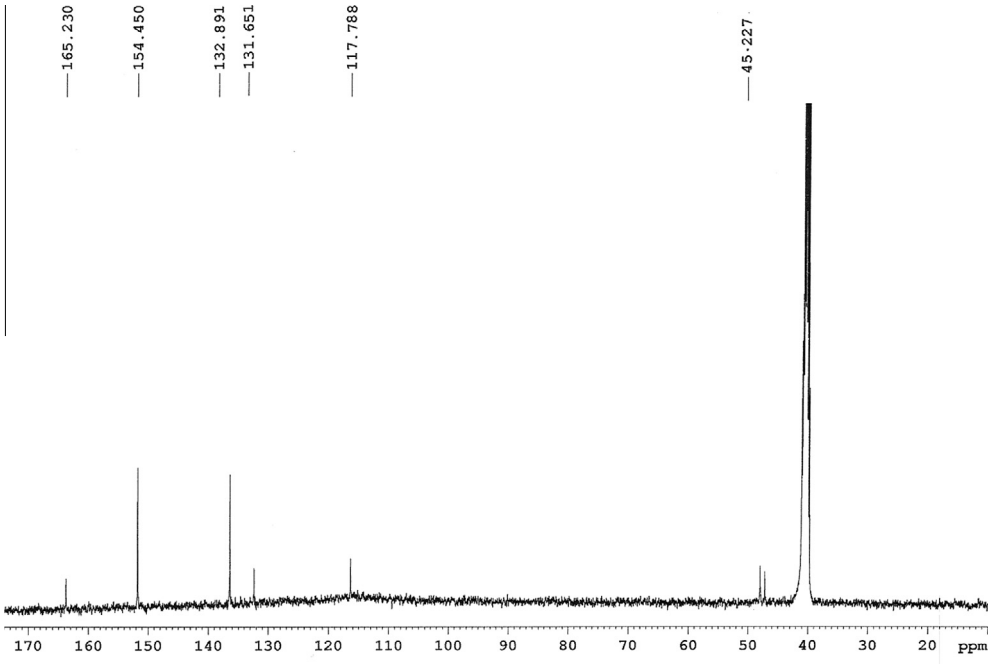

Figure 5 Experimental ^{13}C NMR spectrum of DPBMD.

311 + + G(d,p) level, respectively. The observed NH_2 wagging mode at 910 cm^{-1} agrees well with the calculated wavenumber at 917 cm^{-1} at B3LYP/6-311 + + G(d,p) level. The modes calculated at B3LYP/6-311 + + G(d,p) level show good agreement with experimental value then HF/6-31G(d,p) and B3LYP/6-31G(d,p) level. A combined theoretical and experimental symmetric (3332, 3003 cm^{-1}) and asymmetric (3398, 3276 cm^{-1}) stretching wave number analysis confirms free NH_2 groups in the solid phase FT-IR spectrum of DPBMD.

The C–H stretches of a pyrrole ring and CH_2 group are assigned in the region 3115–3101, 2993–2921 cm^{-1}, respectively. The symmetric and asymmetric CH_2 stretching vibrational bands are assigned at 2979, 3015, 2993 and 2979, 3015, 2993 cm^{-1} in HF/6-31G(d,p), B3LYP/6-31G(d,p),

Please cite this article in press as: Rawat, P., Singh, R.N. Synthesis, spectral analysis and study of antimicrobial activity of 2,5-diformyl-1*H*-pyrrole bis(methan-1-yl-1-ylidene)dimalonohydrazone. Arabian Journal of Chemistry (2014), http://dx.doi.org/10.1016/j.arabjc.2014.10.050

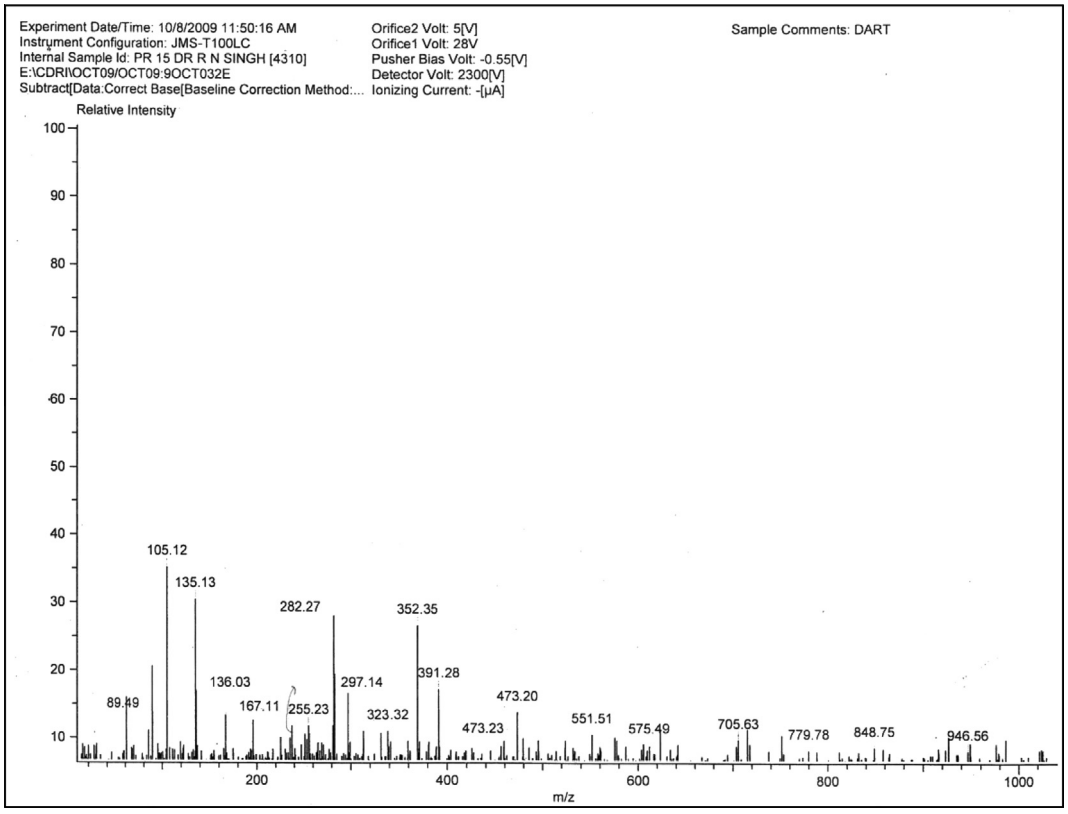

Figure 6 Experimental mass spectrum of DPBMD.

B3LYP/6-311 + + G(d,p) level, respectively. The observed scissoring and wagging modes of CH_2 group at 1420, 1301 cm^{-1}, correspond well to the calculated wavenumber 1400 and 1302 cm^{-1}, in B3LYP/6-311 + + G(d,p) level, respectively. The rocking and twisting vibrations of CH_2 group are assigned at 1269, 803 cm^{-1} (HF/6-31G(d,p)), 1232, 778 cm^{-1} (B3LYP/6-31G(d,p)) and 1226, 776 cm^{-1} (B3LYP/6-311 + + G(d,p)), with very low intensity in PED.

The investigated molecule DPBMD contains four carbonyl groups (>C9═O10, C12═O13, C22═O23, C19═O20). The observed stretching vibration of carbonyl group ($\nu_{C═O}$) at 1679, 1618 cm^{-1} matches well with the calculated wavenumber at 1705, 1646 cm^{-1} in theoretical IR-spectrum. The observed νC12═O13 and νC22═O23 is appears at lower wavenumber than νC9═O10, νC19═O20 due to the involvement of C12═O13 and C22═O23 in intramolecular hydrogen boding with N18–H37/N8–H13. Therefore, the red shift is observed in νC12═O13/νC22═O23 compared with the other C9═O10/C19═O20 group indicates the involvement of the C12═O13/C22═O23 carbonyl group in intramolecular H-bonding. The calculated wavenumber at 1504, 1472, 1458 cm^{-1} exhibits the C═C stretches of pyrrole in HF/6-31G(d,p), B3LYP/6-31G(d,p), B3LYP/6-311 + + G(d,p) level respectively, in the theoretical IR spectrum. The C–C stretches are assigned at 1504, 1472, 1458 cm^{-1} with 8%, 8% contribution in PED.

The observed C═N stretching vibration ($\nu_{C═N}$) at 1586 cm^{-1} agrees with the calculated wavenumber at 1599 cm^{-1} in the theoretical IR spectrum at B3LYP/6-311 + + G(d,p) level. The presence of $\nu_{C═N}$ confirms the Schiff base (C═N) linkage in the product molecule DPBMD. The observed $\nu_{C═N}$ at 1586 cm^{-1} also agrees well with the reported absorption band in literature (Singh and Rawat, 2013). The C–N out-of-plane deformation mode associated with azomethine group is assigned at 917, 916, 910 cm^{-1} in B3LYP/6-311 + + G(d,p), B3LYP/6-31G(d,p), HF/6-31G(d,p), level, respectively. This calculated mode at B3LYP/6-311 + + G(d,p) level show good agreement with experimental value at 906 cm^{-1} then HF/6-31G(d,p) and B3LYP/6-31G(d,p) level. The N–N stretching vibration ($\nu_{N–N}$) is calculated at 1096, 1113, 1121 cm^{-1} in B3LYP/6-311 + + G(d,p), B3LYP/6-31G(d,p), HF/6-31G(d,p), level, respectively, and correlate well with the observed wavenumber at 1075 cm^{-1} in the experimental FT-IR spectrum.

3.3.2. ^{1}H NMR and UV–Vis spectroscopy

The calculated and experimental ^{1}H and ^{13}C chemical shifts (δ/ppm) of DPBMD in DMSO solvent are given in Supplementary Tables S5 and S6 and shown in Figs. 4 and 5, respectively. In experimental ^{1}H NMR spectrum, the observed singlet chemical shifts at 5.849 ppm confirms free NH_2 groups in the solid phase FT-IR spectrum of DPBMD. The observed chemical shift at 8.884 ppm as singlet for ─CH═N─proton confirms formation of dihydrazone molecule. Additional support for the structure of the synthesized compound was provided by its ^{13}C NMR spectrum, in which chemical shift values of azomethine carbon atom found to be at 132.89 ppm (**C**H═N), corroborated well with reported hydrazone compound (Singh and Rawat, 2013). Both *ab initio* HF and DFT(B3LYP) methods did not produced much differences in calculated chemical

Table 2 Calculated and experimental electronic excitations of Conformer I for DPBMD: E/eV, oscillatory strength (f), (λ_{max}/nm) at TD-DFT 6-311++G(d,p) level.

S. No.	Excitations	E (eV)	(f)	λ_{max} calcd	λ_{max} obs	Assignment
Gas phase						
1	92→93 (H→L)	3.4807	0.9325	356.20	406	$n\rightarrow\pi^*$
2	92→94 (H-1→L+1)	4.3385	0.0357	285.78		
3	77→81(H–2→L+1)	5.1054	0.6076	242.85	269	$\pi\rightarrow\pi^*$
Solvent phase						
1	92→93 (H→L)	3.2425	0.9299	382.37	406	$n\rightarrow\pi^*$
2	92→94 (H-1→L+1)	4.3031	0.0645	288.13		
3	77→81(H–2→L+1)	4.9502	0.4270	261.25	269	$\pi\rightarrow\pi^*$

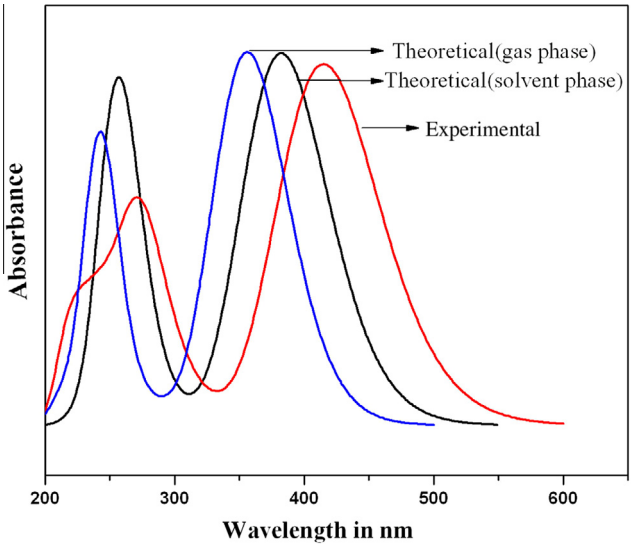

Figure 7 Comparison between experimental and theoretical UV–Visible spectrum of Conformer I for DPBMD.

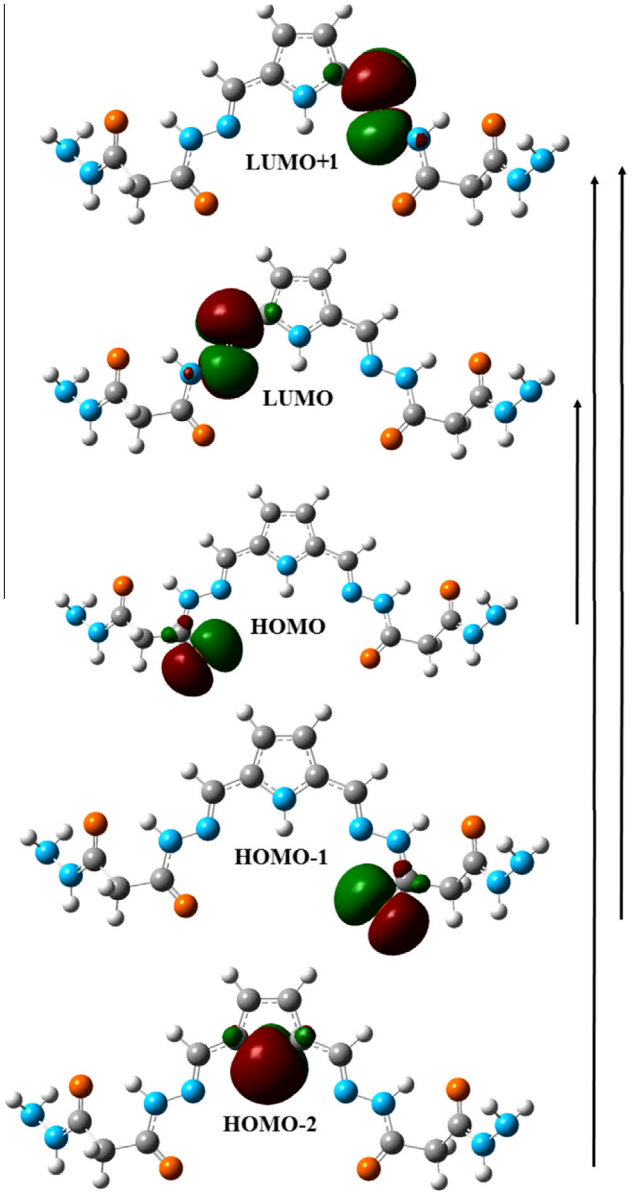

Figure 8 The molecular orbital plot of Conformer I for DPBMD.

shifts of the studied compound. There is a good agreement between experimental and theoretical chemical shift results for the DPBMD. The performances of the B3LYP method with respect to the prediction of the chemical shifts within the molecule were quite close. The molecular mass of the compound was confirmed by Mass spectrometry analysis and given in Fig. 6. The presence of a molecular ion peak at 352 confirmed the formation of the product. The ^{1}H NMR and Mass spectra of compound (6) shown in Scheme 1 are given in Supplementary Fig. S2 and S3, respectively. The disappearance of NH_2 peak in ^{1}H NMR spectrum of (6) indicates that cyclic compound is formed. Again the presence of a molecular ion peak at 439.15 confirmed the formation of the product (6).

The nature of the transitions and electronic excitations of high oscillatory strength calculated at B3LYP/6-311++G(d,p) and (B3LYP/6-31G(d,p), HF/6-31G(d,p)) level are listed in Table 2 and Supplementary Table S7, respectively, with the experimental observations. The comparison between experimental and theoretical UV–Visible spectra for DPBMD is shown in Fig. 7 and molecular plot is shown in Fig. 8. The

Please cite this article in press as: Rawat, P., Singh, R.N. Synthesis, spectral analysis and study of antimicrobial activity of 2,5-diformyl-1*H*-pyrrole bis(methan-1-yl-1-ylidene)dimalonohydrazone. Arabian Journal of Chemistry (2014), http://dx.doi.org/10.1016/j.arabjc.2014.10.050

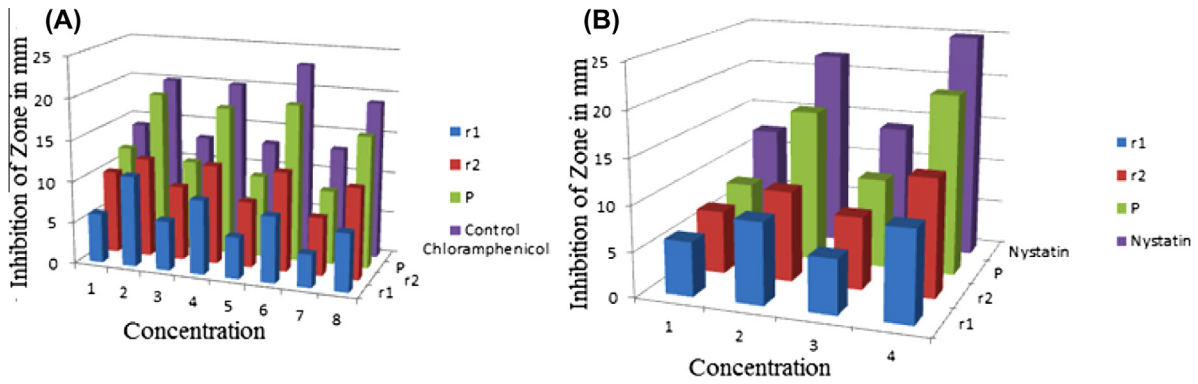

Figure 9 Bar diagrams represent the inhibition of zone in mm for (A) bacterial and (B) fungal strains.

Table 3 Calculated ε_{HOMO}, ε_{LUMO}, energy band gap (ε_L–ε_H), chemical potential (μ), electronegativity (χ), global hardness (η), global softness (S) and global electrophilicity index (ω) for (**1** = 2,5 diformyl-1*H*-pyrrole), (**2** = malonic acid dihydrazide), and DPBMD (conformer I), electrophilicity based charge transfer (ECT) for reactant system [(**1**)↔(**2**)]/[(2,5 diformyl-1*H*-pyrrole)↔(malonic acid dihydrazide)].

	ε_H	ε_L	ε_H–ε_L	$\mu = -\chi$	η	S	ω	ECT
(1)	−6.8410	−2.3647	4.4763	4.6028	2.2381	0.2233	4.7329	1.0620
(2)	−6.7569	0.0185	6.7754	3.3692	3.3877	0.1475	1.6754	
(DPBMD)	−5.0577	−1.4351	3.6226	3.2464	1.8113	0.2760	2.9092	

ε_H, ε_L, (ε_H–ε_L), μ, χ, η, ω/eV and S/eV.

Table 4 Calculated dipole moment (μ_0), polarizability ($|\alpha_0|$), anisotropy of polarizability ($\Delta\alpha$), first hyperpolarizability (β_0) and their components at B3LYP/6-311++G(d,p) level of Conformer I.

Dipole moment		Polarizability		First hyperpolarizability	
μ_x	−0.014	α_{xx}	429.95	β_{xxx}	−0.2303
μ_y	3.251	α_{yy}	12.37	β_{xxy}	−707.2
μ_z	0.375	α_{zz}	283.64	β_{xyy}	−0.3664
μ_0	3.273	$\|\alpha_0\|$	35.862	β_{yyy}	−64.51
		$\Delta\alpha$	123.03	β_{xxz}	−4.327
				β_{xyz}	130.38
				β_{yyz}	8.922
				β_{xzz}	−28.67
				β_{yzz}	100.98
				β_{zzz}	−1.164
				β_0	5.8002

calculated electronic excitation at λ_{max} = 347 nm, f = 0.867 (HF/6-31G(d,p)), 376 nm, f = 0.932 (B3LYP/6-31G(d,p)), 382 nm, f = 0.9299 (B3LYP/6-311++G(d,p)) level in gas phase UV–Visible of DPBMD. The calculated electronic transition at B3LYP/6-311++G(d,p) level of DPBMD in solvent phase matches well the experimental absorption in UV–Visible spectrum. The first observed electronic excitation at λ_{max} = 406 at B3LYP/6-311++G(d,p) level of DPBMD corroborates well with the calculated λ_{max} = 382 value. The second observed λ at 269 nm agrees well with the aggregate of two electronic transitions calculated at λ = 261 nm, f = 0.4270. This calculated electronic transitions at B3LYP/6-311++G(d,p) level show good agreement with the experimental value. Therefore, the observed λ_{max} are red shifted up to ~24 nm compared with the calculated λ_{max} in the theoretical UV–Visible spectrum. On the basis of molecular orbital coefficients analysis the nature of both electronic excitations is assigned as n→π* and π→π* (see Fig. 8).

3.4. Natural bond orbitals (NBO) analysis

Natural bond orbital (NBO) analysis is an important tool for studying hybridization, covalency effects, hydrogen-bonding and van der Waals interactions (Weinhold and Landis, 2005). The intramolecular interaction are formed by the orbital overlap between σ(C—C), σ*(C—C), π(C—C), π*(C—C) bond orbital which results intermolecular charge transfer (ICT) causing stabilization of the system. These interactions are observed as increase in electron density (ED) in C—C antibonding orbital that weakens the respective bonds. These intramolecular charge transfer (σ→σ*, π→π*) can induce large nonlinearity of the molecule. Second-order perturbation theory analysis of the Fock matrix in NBO basis for DPBMD is presented in Supplementary Table S8. The interactions π(C2–C3)→π*(C4–C5), π(C2–C3)→π*(C4–C5), are responsible for conjugation of respective π-bonds in pyrrole ring due to the high electron density at π bonds (1.721), low density at π* bonds (0.411) and stabilized the molecule with energy in the region 19.48 kcal/mol. In same way, the conjugation of respective π-bonds in with azomethine frame work can be explained due to the π→π* interactions. The interactions π(N7–C6)→π*(C2–C3), π(N17–C16)→π*(C3–C5) demonstrate strong π–electron delocalization toward pyrrole ring from azomethine group stabilized the molecule with $E^{(2)}_{max}$ ~10.28 kcal/mol. For DPBMD, n(N14/N24), n(N18) of the NBO conjugated with π*(C12–O13/C22–O23), σ(C19–O20) leads to an enormous stabilization of 64.10 and 17.28 kcal/mol,

Please cite this article in press as: Rawat, P., Singh, R.N. Synthesis, spectral analysis and study of antimicrobial activity of 2,5-diformyl-1*H*-pyrrole bis(methan-1-yl-1-ylidene)dimalonohydrazone. Arabian Journal of Chemistry (2014), http://dx.doi.org/10.1016/j.arabjc.2014.10.050

Table 5 The antimicrobial activity of reactants (r1, r2) and product (P) at different concentration. (r1 = 2,5 diformyl-1*H*-pyrrole), (r2 = malonic acid dihydrazide), and (P = DPBMD).

Compd	Zone of inhibition (mm)							
	Gram positive				Gram negative			
	S. aureus		*S. pyogenes*		*E. coli*		*P. aeruginosa*	
	μg/ml		μg/ml		μg/ml		μg/ml	
Antibacterial activity								
	100	200	100	200	100	200	100	200
r1	6	11	6	9	5	8	4	7
r2	10	12	9	12	8	12	7	11
P	12	19	11	18	10	19	9	16
Control chloramphenicol	14	20	13	20	13	23	13	19
Compd	*C. albicans* μg/ml				*A. niger* μg/ml			
Antifungal activity								
	100		200		100		200	
r1	6		9		6		10	
r2	7		10		8		13	
P	8		17		10		20	
Nystatin	12.5		22		14		25	

respectively. This strong stabilization denotes the larger delocalization. This highest interaction around the ring can induce the large bioactivity in the compound.

3.5. Frontier molecular orbitals (FMOs), electronic descriptors and Molecular Electrostatic Potential Surface (MEPS)

Two new orbitals are formed by the interaction of two atomic (or) molecule. Two interacting molecular orbitals are generally the highest energy occupied molecular orbital (HOMO) and lowest unoccupied molecular orbital (LUMO) of the compound. These molecular orbital plays an important role in the optical and electric properties, as well as in quantum chemistry and UV–Vis spectra. A molecule with a small frontier orbital gap is generally associated with a high chemical reactivity, low kinetic stability and is also termed as soft molecule. The calculated energy values of HOMO, LUMO and band gap are

HOMO = −6.634 LUMO = 1.988 eV, Band gap = 8.622 eV, at HF/6-31G(d,p)

HOMO = −5.057 eV LUMO = −1.435 eV, Band gap = 3.622 eV, at B3LYP/6-31G(d,p)

HOMO = −5.507 eV LUMO = −1.941 eV, Band gap = 3.566 eV, at B3LYP/6-311 + + G(d,p)

The lower value of energy gap explains the charge transfer interactions taking place within the molecule, which influences the biological activity of the molecule. The calculated bad gap at B3LYP/6-31G(d,p) and B3LYP/6-311 + + G(d,p) level is lower than HF/6-31g(d,p). The narrow energy gap between HOMO and LUMO facilitates intra molecular charge transfer which makes the material to be NLO active. The chemical reactivity and site selectivity of the molecular systems have been determined on the basis of Koopman's theorem (Geerlings et al., 2003). Global reactivity descriptors successfully predicts global reactivity trends (Singh and Rawat, 2013) and given in Table 3. Electrophilic charge transfer (ECT) = $(\Delta N_{max})_A - (\Delta N_{max})_B$ (Rawat and Singh, 2014a,b; Singh et. al., 2013, 2015) is defined as the difference between the ΔN_{max} values of interacting molecules. ECT of DPBMD is calculated as 1.062, i.e., ECT > 0 for reactant system [(**1**)↔(**2**)], which indicates that charge flows from (**2**) to (**1**). Therefore, (**1**) acts as electron acceptor (electrophile) and (**2**) as electron donor (nucleophile). The global electrophilicity index (ω = 2.909 eV) of conformer I of DPBMD shows that this behaves as a strong electrophile.

The electrostatic potential surface (MEPS) of DPBMD is shown in Fig. 2. The MEPS has three projections, one in molecular plane and two in perpendicular planes. The DPBMD molecule has nine oxygen atoms. The Mulliken atomic charge on azomethine nitrogen (>CH═N7─/N17), (>CH═N**N**18H/**N**8H) are 0.097 and −0.128. The Mulliken atomic charge 0.105 on pyrrolic nitrogen atom (N1) is more positive then N7 and N17 atoms. The negative charge in hydrazide N14H33/N24H40 (CO**N**HNH2) nitrogen atom is more located as compared to the nitrogen N8 and N18. The largest negative charges −0.341 is located on the nitrogen atom N15/N25 of amino group than other nitrogen atom. It is clear that electrophilic reaction occur at NH_2 group. However hydrogens of pyrrolic NH possess more positive charge (0.389) than hydrogen atoms of NH_2 group (0.264).

3.6. Static dipole moment (μ_0), mean polarizability ($|\alpha_0|$), anisotropy of polarizability ($\Delta\alpha$) and first hyperpolarizability (β_0)

Theoretical calculations on molecular hyperpolarizability β is quite useful both in understanding the relationship between the molecular structure and nonlinear optical properties as hyperpolarizability is difficult task to measure directly computational calculation is an alternate choice (Kleinmann, 1962). The first hyperpolarizability (β_0) of this novel molecular

system, and related properties ($|\alpha_0|$ and $\Delta\alpha$) are calculated at B3LYP/6-311++G(d,p), and (B3LYP/6-31G(d,p), HF/6-31G(d,p)) level based on the finite-field approach and their calculated values are given in Table 4 and Table S9, respectively. The first hyperpolarizability (β_0) of DPBMD are calculated as 5.42×10^{-30}, 5.71×10^{-30} esu HF/6-31G(d,p), B3LYP/6-31G(d,p) and 5.80×10^{-30} B3LYP/6-311++G(d,p) level. In this study, *p*-nitroaniline (*p*-NA) is chosen as a reference molecule (Jug et al., 2003). The *p*-NA is one of the prototypical molecules used in the study of the NLO properties of molecular systems (for *p*-NA, $\beta_0 = 11.54\times10^{-30}$ esu). The investigated molecule would show non-linear optical response and might be used in non-linear optical (NLO) applications.

3.7. Evaluation of antimicrobial activity

The compound and reactants reported in Table 5 showed a good antibacterial and antifungal activity. Fig. 9 shows bar diagram for representation of zone inhibition in mm of (a) against bacterial strains (b) against fungal strains. The product PDBO shows good antibacterial activity in comparison to 2,5-diformyl-1*H*-pyrrole and malonic acid dihydrazide. The product DPBMD was found more active against gram positive *S. aureus* and *S. pyogenes* bacterial strain at μg/ml concentration. The reactant (r1) found in most of the case less active against both gram positive and gram negative bacteria. The results of preliminary antifungal activity screening reveals that DPBMD has significant effect on *C. albicans* and *A. niger*, even at 100 μg/ml concentration, though the best results comes only at 200 μg/ml, respectively. In all cases the assayed substances showed an activity level against bacterial and fungal lower than that of chloramphenicol and Nystatin, the reference drug.

4. Conclusions

The synthesized compound 2,5-diformyl-1*H*-pyrrole bis(methan-1-yl-1-ylidene)dimalonohydrazone has been characterized by various experimental spectroscopic techniques. Theoretical calculations were performed by *ab initio* RHF and density functional theory (DFT) method, using B3LYP/6-31G(d,p) and B3LYP/6-311+G(d,p) basis sets. The vibrational frequencies have been calculated and scaled values are comparable with experimental FT-IR spectrum. The scaled calculated vibrational frequencies at B3LYP/6-311++G(d,p) level shows excellent agreement with experimental wavenumbers. A combined experimental and theoretical stretching wave numbers symmetric (3003, 3332 cm^{-1}) and asymmetric (3276, 3398 cm^{-1}) analysis confirms free NH_2 groups in DPBMD. A found electronic excitations are $n\rightarrow\pi^*$ and $\pi\rightarrow\pi^*$ in nature. Involvement of nitrogen loin pairs of electrons leads to an enormous stabilization of DPBMD molecule. The calculated electronic descriptor analysis indicates that studied molecule is a good precursor for heterocyclic synthesis and as ligand for metal complex formation. First hyperpolarizability ($\beta_0 = 5.42/5.71/5.80\times10^{-30}$ esu) at *ab initio* RHF, B3LYP/6-31G(d,p) and B3LYP/6-311+G(d,p) level of DPBMD has been computed to evaluate non-linear optical (NLO) response. On the basis of first hyperpolarizability ($\beta_0 = 5.42/5.71/5.80\times10^{-30}$ esu), we conclude that title compound DPBMD can be used as an attractive material for non-linear optical (NLO) applications. The preliminary bioassay suggested that the DPBMD exhibits good antibacterial and fungicidal activity.

Acknowledgements

The authors are thankful to the National Council of Educational Research and Training and Department of Science and Technology, New Delhi – India for providing the financial support.

Appendix A. Supplementary data

Supplementary data associated with this article can be found, in the online version, at http://dx.doi.org/10.1016/j.arabjc.2014.10.050.

References

Adam, M.S.S., 2014. Synthesis and characterization of novel bis(diphenylphosphino)-oxalyl and (substituted) malonyldihydrazones: P,N,N,P-tetradentate complexes of an oxalyl derivative with Cu(II), Pd(II), and Mn(II). Monatsh. Chem. 145, 435–445.

Alamuoye, A.E., Nwabueze, J.N., 2014. Synthesis and characterization of the complexes of acetone succinyldihydrazone and fufuraldehydesuccinyldihydrazone with Ni(II) sulphate and acetate. Int. J. Inorg. Bioinorg. Chem. 4, 1–4.

Alonso, R., Bermejo, E., Carballo, R., Castineiras, A., Perez, T., 2002. The supramolecular chemistry of thiosemicarbazones derived from pyrrole: a structural view. J. Mol. Struct. 606, 153–173.

Bacchi, A., Bonardi, A., Carcelli, M., Mazza, P., Pelagatti, P., Pelizzi, C., Pelizzi, G., Solinas, C., 1998. Organotin complexes with pyrrole-2,5-dicarboxaldehyde bis(acylhydrazones). J. Inorg. Biochem. 69, 101–112.

Bader, R.F.W., Cheeseman, J.R., In; AIMPAC Ed., 2000.

Balasubramanian, N., Pradeep, K., Deepika, S., 2010. Biological activities of hydrazide derivatives in the new millennium. Acta Pharm. Sci. 52, 169–180.

Battaglia, L.P., Corradi, A.B., Pelizzi, C., Pelosi, G., Tarasconi, P., 1990. Chemical and structural investigations on bismuth complexes of 2,6-di-acetylpyridine bis(2-thenoylhydrazone) and 2,6-diacetylpyridine bis(thiosemicarbazone). J. Chem. Soc., Dalton Trans., 3857–3860.

Bruni, A.T., Pereira, V.B., 2012. In: Dr. Tomofumi Tada (Ed.), Quantum Chemistry and Chemometrics Applied to Conformational Analysis, Quantum Chemistry – Molecules for Innovations. InTech, ISBN 978-953-51-0372-1, pp. 15–28, available from: http://www.intechopen.com/books/quantum-chemistry-moleculesfor-innovations/quantum-chemistry-and-chemometrics-applied-to-conformational-analysis.

Ditchfield, R., 1972. Molecular orbital theory of magnetic shielding and magnetic susceptibility. J. Chem. Phys. 56, 5688–5691.

Eshkourfu, R., Čobeljić, B., Vujčić, M., Turel, I., Pevec, A., Sepčić, K., Zec, M., Radulović, S., Srdić-Radić, T.D., Katarina, M., DušanSladić, A., 2011. Synthesis, characterization, cytotoxic activity and DNA binding properties of the novel dinuclearcobalt(III) complex with the condensation product of 2-acetylpyridine and malonic acid dihydrazide. J. Inorg. Biochem. 105, 1196–1203.

Frisch, M.J. et al, 2010. Gaussian 09 (Revision B9). Gaussian Inc, Pittsburgh.

Computer program Gauss View 3.09, Ver. 2, 2003. Gaussian Inc, PA, Pittsburgh.

Geerlings, P., De Proft, F., Langenaeker, W., 2003. Conceptual density functional theory. Chem. Rev. 103, 1793–1873.

John, D., Curry, M.A.R., Busch, D.H., 1967. Metal complexes derived from substituted hydrazones of 2,6-diacetylpyridine. Inorg. Chem. 6, 1570–1574.

Jug, K., Chiodo, S., Calaminici, P., Avramopoulos, A., Papadopoulos, M.G., 2003. Electronic and vibrational polarizabilities and hyperpolarizabilities of azoles: a comparative study of the structure–polarization relationship. J. Phys. Chem. A 107, 4172–4183.

Kleinmann, D.A., 1962. Nonlinear dielectric polarization in optical media. Phys. Rev. 126, 1977.

Knizhnikova, V.A., Borisovab, N.E., Yurashevicha, N.Ya., Popovaa, L.A., Chernyadvc, A.Yu., Zubreichuka, Z.P., Reshetovab, M.D., 2007. Pincer ligands based on α-amino acids: I. Synthesis of polydentate ligands from pyrrole-2,5-dicarbaldehyde. Russ. J. Org. Chem. 43, 855–860.

Lal, R.A., Chakraborty, J., Kumar, A., Bhaumik, S., Nath, R.K., Ghosh, D., 2004. A study on heterobimetallic chemistry of polyfunctional bis(2-hydroxy-1-naphthaldehyde)malonoyldihydrazone: Dioxouranium(VI), dioxomolybdenum(VI), zinc(II), copper(II), nickel(II) and cobalt(II) complexes. Indian J. Chem. 43A, 516–526.

Lal, R.A., Choudhury, S., Ahmed, A., Borthakur, R., Asthana, M., Kumar, A., 2010. Synthesis of homobimetallic molybdenum (VI) complex of bis (2-hydroxy-1-naphthaldehyde) malonoyldihydrazone and its reaction with electron and proton bases. Spectrochimica Acta Part A 75, 212–224.

Leonid, D.P., Morozov, A.N., Shcherbakov, Igor N., Tupolova, Yu P., Lukov, V.V., Kogan, V.A., 2009. Metal complexes with polyfunctional ligands based of bis(hydrazones) of dicarbonyl compounds. Russ. Chem. Rev. 78, 643.

Martin, J.M.L., Alsenoy, V., Alsenoy, C.V., 1995. Gar2ped. University of Antwerp.

Popov, L.D., Levchenkov, S.I., Shcherbakov, I.N., Kiskin, M.A., Borisova, N.E., Tsaturyan, A.A., Kogan, V.A., 2013. Crystal structure of bis-isonicotinoylhydrazone of 2,5-diformylpyrrole. J. Struct. Chem. 54, 592–597.

Popov, L.D., Morozov, A.N., Shcherbakov, I.N., Tupolova, Yu.P., Lukov, V.V., Kogan, V.A., 2009. Metal complexes with polyfunctional ligands based of bis(hydrazones) of dicarbonyl compounds. Russ. Chem. Rev. 78, 643–658.

Pulay, P., Fogarasi, G., Pang, F., Boggs, J.E., 1979. Systematic ab initio gradient calculation of molecular geometries, force constants, and dipole moment derivatives. J. Am. Chem. Soc. 101, 2550.

Ramalingam, S., Periandy, S., Narayanan, B., Mohan, S., 2010. FTIR and FTRaman spectroscopic investigation of 2-bromo-4-methylaniline using ab initio HF and DFT calculations. Spectrochimicaacta Part A 76, 84–92.

Rawat, P., Singh, R.N., 2014a. Evaluation of molecular assembly, spectroscopic interpretation, intra-/inter molecular hydrogen bonding and chemical reactivity of two pyrrole precursors. J. Mol. Struc. 1075, 462–470.

Rawat, P., Singh, R.N., 2014b. Spectral analysis, structural elucidation and evaluation of chemical reactivity of synthesized ethyl-4-[(2-cyano-acetyl)-hydrazonomethyl]-3,5-dimethyl-1H-pyrrole-2-carboxylate through experimental studies and quantum chemical calculations. J. Mol. Struc. 1074, 201–212.

Safoklov, B.B., Atovmyan, E.G., Nikonova, L.A., 2002. Characteristic features of intra- and intermolecular interactions in crystals of pyrrole-2-carbaldehyde isonicotinoylhydrazone and its hydrate. Russ. Chem. Bull. 51, 2224–2229.

Sedaghat, T., Monajjemzadeh, M., 2011. Some new organotin(IV) schiff base adducts: Synthesis, spectroscopic characterization and thermal studies. J. Iran. Chem. Soc. 8, 477–483.

Silverstein, R.M., Webster, F.X., 1963. Spectrometric Identification of Organic Compounds, 6th ed. Jon Wiley Sons Inc, New York.

Singh, R.N., Rawat, P., 2013. Spectral analysis, structural elucidation, and evaluation of both nonlinear optical properties and chemical reactivity of a newly synthesized ethyl-3,5-dimethyl-4-[(toluenesulfonyl)-hydrazonomethyl]-1H pyrrole-2-carboxylate through experimental studies and quantum chemical calculations. J. Mol. Struct. 1054–1055, 65–75.

Singh, R.N., Rawat, P., Sahu, S., 2013. Investigation of spectroscopic, structural and non-linear optical properties of ethyl 3,5-dimethyl-4-[(benzenesulfonyl)-hydrazonoethyl]-1H-pyrrol-2-carboxylate. J. Mol. Struct. 1054–1055, 123–133.

Singh, R.N., Rawat, P., Sahu, S., 2015. Vibrational spectra, electronic absorption, nonlinear optical properties, evaluation of bonding, chemical reactivity and thermodynamic properties of ethyl 4-(1-(2-(hydrazinecarbonothioyl)hydrazono) ethyl)-3,5-dimethyl-1H-pyrrole-2-carboxylate molecule by ab initio HF and density functional methods. Spectrochimica Acta Part A 135, 1162–1168.

Tomasi, J., Mennucci, B., Cammi, R., 2005. Quantum mechanical continuum solvation models. Chem. Rev. 105, 2999–3093.

Wardell, S.M.S.V., De Souza, M.V.N., Wardell, J.L., 2006. Pyrrole-2-carbaldehyde isonicotinoylhydrazone monohydrate redetermined at 120 K. Acta Crystallogr. C62, o47–o49.

Weinhold, F., Landis, C.R., 2005. Valency and Bonding: A Natural Bond Orbital Donor–Acceptor Perspective. Cambridge University Press, Cambridge, New York, Melbourne, pp. 215–274.

Wolinski, K., Hinton, J.F., Pulay, P., 1990. Efficient implementation of the gauge-independent atomic orbital method for NMR chemical shift calculations. J. Am. Chem. Soc. 112, 8251–8260.

Yi-Gui, Wang., 2009. Examination of DFT and TDDFT methods I. J. Phys. Chem. A 113, 10867–10872.

Zoubi, W.Al., Kandil, F., Chebani, M.K., 2012. Synthesis of macrocyclic schiff bases based on pyridine-2,6-dicarbohydrazide and their use in metal cations extraction. Org. Chem. Curr. Res. 1, 1–7.

Please cite this article in press as: Rawat, P., Singh, R.N. Synthesis, spectral analysis and study of antimicrobial activity of 2,5-diformyl-1*H*-pyrrole bis(methan-1-yl-1-ylidene)dimalonohydrazone. Arabian Journal of Chemistry (2014), http://dx.doi.org/10.1016/j.arabjc.2014.10.050